Am J Physiol Heart Circ Physiol 322: H1032–H1043, 2022.
First published April 29, 2022; doi:10.1152/ajpheart.00664.2021

american physiological society

AMERICAN JOURNAL OF PHYSIOLOGY
HEART AND CIRCULATORY PHYSIOLOGY

RESEARCH ARTICLE

Energetics and Metabolism

α-Tubulin acetylation on lysine 40 controls cardiac glucose uptake

Edith Renguet,[1]* Marine De Loof,[1]* Natacha Fourny,[1] Audrey Ginion,[1] Caroline Bouzin,[2] Christian Poüs,[3,4] Sandrine Horman,[1] Christophe Beauloye,[1,5] Laurent Bultot,[1] and Luc Bertrand[1]

[1]*Institut de Recherche Expérimentale et Clinique, Pole of Cardiovascular Research, Université catholique de Louvain, Brussels, Belgium;* [2]*Institut de Recherche Expérimentale et Clinique, IREC Imaging Platform (2IP), Université catholique de Louvain, Brussels, Belgium;* [3]*INSERM UMR-S-1193, Université Paris-Saclay, Châtenay-Malabry, France;* [4]*AP-HP, Biochimie-Hormonologie, Hôpital Antoine Béclère, Clamart, France; and* [5]*Division of Cardiology, Cliniques Universitaires Saint-Luc, Brussels, Belgium*

Abstract

Our group previously demonstrated that an excess of nutrients, as observed in diabetes, provokes an increase in cardiac protein acetylation responsible for a reduced insulin-stimulated translocation of the glucose transporter GLUT4 to the plasma membrane. The acetylated proteins involved in this event have yet not been identified. α-Tubulin is a promising candidate as a major cytoskeleton component involved, among other things, in the translocation of GLUT4-containing vesicles from their intracellular pools toward the plasma membrane. Moreover, α-tubulin is known to be acetylated, Lys40 (K40) being its best characterized acetylated residue. The present work sought to evaluate the impact of α-tubulin K40 acetylation on cardiac glucose entry, with a particular interest in GLUT4 translocation. First, we observed that a mouse model of high-fat diet-induced obesity presented an increase in cardiac α-tubulin K40 acetylation level. We next showed that treatment of insulin-sensitive primary cultured adult rat cardiomyocytes with tubacin, a specific tubulin acetylation inducer, reduced insulin-stimulated glucose uptake and GLUT4 translocation. Conversely, decreasing α-tubulin K40 acetylation by expressing a nonacetylable dominant form of α-tubulin (mCherry α-tubulin K40A mutant) remarkably intensified insulin-induced glucose transport. Finally, mCherry α-tubulin K40A expression similarly improved glucose transport in insulin-resistant cardiomyocytes or after AMP-activated protein kinase activation. Taken together, our study demonstrates that modulation of α-tubulin K40 acetylation level affects glucose transport in cardiomyocytes, offering new putative therapeutic insights regarding modulation of glucose metabolism in insulin-resistant and diabetic hearts.

NEW & NOTEWORTHY Acetylation level of α-tubulin on K40 is increased in the heart of a diet-induced mouse model of type 2 diabetes. Pharmacological stimulation of α-tubulin K40 acetylation lowers insulin-mediated GLUT4 vesicles translocation to the plasma membrane, reducing glucose transport. Expressing a nonacetylable dominant form of α-tubulin boosts glucose uptake in both insulin-sensitive and insulin-resistant cardiomyocytes.

acetylation; cardiac metabolism; glucose uptake; GLUT4; tubulin

INTRODUCTION

The heart requires a large amount of energy to sustain its continuous mechanical work. Cardiac energy reserve being limited, the heart needs to constantly adapt its metabolism to the availability of the various circulating substrates to ensure efficient energy production. Under physiological conditions, the heart preferentially uses fatty acids in fasted state and carbohydrates in postprandial state. This metabolic flexibility is essential for optimal cardiac function (1, 2) and is altered in several metabolic diseases, including type 2 diabetes (3, 4). Indeed, the diabetic heart progressively loses its ability to stimulate glucose metabolism in response to insulin and therefore mostly relies on lipids to generate ATP. In the long term, this preferential use of fatty acids becomes deleterious for cardiac function. Among other things, it participates in the development of mitochondrial dysfunction and oxidative stress, lowering ATP production and contractile efficiency (5). Understanding the mechanisms responsible for metabolic inflexibility installment is therefore crucial when considering new therapeutic approaches to prevent cardiac dysfunction during diabetes. From this perspective, elucidation of the regulatory mechanisms controlling glucose utilization and particularly its transport across the plasma membrane, the first limiting step of its catabolism, is of great interest. In cardiomyocytes, stimulation of glucose entry largely depends on the

*E. Renguet and M. De Loof contributed equally to this work.
Correspondence: L. Bertrand (luc.bertrand@uclouvain.be).
Submitted 10 December 2021 / Revised 22 April 2022 / Accepted 22 April 2022

facilitated glucose transporter GLUT4 (6–8). In the basal state, GLUT4 is mostly retained in specialized intracellular vesicles named GLUT4 storage vesicles (GSVs) (9, 10). Insulin secretion in response to a postprandial rise in glycemia leads to a large relocation of GLUT4 to the cell surface by promoting GSVs migration toward the cardiomyocyte periphery and their fusion with the plasma membrane, which results in a strong stimulation of cardiac glucose uptake (11–13).

It is known that an excess of ATP-generating substrates such as fatty acids, ketone bodies, and leucine, as observed in diabetes (14, 15), induces a defect in insulin-dependent GLUT4 translocation in cardiomyocytes (16, 17). We recently demonstrated that such an inhibition can be explained by a rise in protein acetylation (17). With the goal of identifying acetylated proteins potentially involved in glucose uptake inhibition, we hypothesize that tubulin is a promising candidate. α-Tubulin, with its partner β-tubulin, forms the microtubule network used as tracks for GSVs migration from cytoplasmic pools to the plasma membrane (18, 19). Additionally, α-tubulin was the first nonhistone protein discovered to be acetylated, Lys-40 (K40) being its best-characterized acetylation site (20, 21) (Fig. 1*A*). Mostly studied in neurobiology, α-tubulin K40 acetylation level is controlled by a specific cytosolic acetyltransferase called α-tubulin acetyltransferase (α-TAT) (22, 23), whereas two cytosolic deacetylases, HDAC6 and SIRT2 were identified to manage α-tubulin deacetylation, the first one being considered as the predominant α-tubulin deacetylase (24, 25). Intensive investigation has been performed to elucidate the impact of α-tubulin K40 acetylation on microtubule stability (26–29). Results remain controversial but recent publications suggest that α-tubulin acetylation on K40 regulates microtubule dynamics by weakening interactions between protofilaments, the linear arrangements of subunits that constitute the microtubule wall (30–32). On the other hand, it has been demonstrated that an intact microtubule network is required for proper GLUT4 translocation (33). But, as far as we know, the role of α-tubulin acetylation on GLUT4 translocation has never been assessed. Here, we show that α-tubulin K40 acetylation levels increase in the heart of a high-fat diet (HFD)-mediated mouse model of type 2 diabetes. We also demonstrate that increasing α-tubulin K40 acetylation using the pharmacological compound tubacin reduces GLUT4 translocation, glucose uptake, and glycolysis upon insulin stimulation. On the contrary, decreasing α-tubulin K40 acetylation by overexpressing a nonacetylable dominant form of α-tubulin stimulates glucose transport and metabolism in both control and insulin-resistant conditions, uncovering the possibility of targeting α-tubulin K40 acetylation to correct defective glucose uptake in the heart.

MATERIALS AND METHODS

Animal Care

Animal handling was approved by local authorities (Comité d'éthique Facultaire pour l'Expérimentation Animale, 2016/UCL/MD/027 and 2021/UCL/MD/015) and conformed to the Guide for the Care and Use of Laboratory Animals published by the National Institutes of Health (NIH Publication No. 85-23, Revised 1996).

High-Fat Diet Mouse Model

Eight-week-old C57BL6/N male mice (Janvier laboratories) were fed 4 mo with a regular diet (chow diet, CD, Safe diets, Safe A04, No. U822G10R) or a high-fat diet (HFD) (Research diet, No. D12492) before euthanasia. Mice have been randomly distributed into one or the other diet group and their weight was followed weekly.

Glucose Tolerance Test and Euthanasia

After 4 mo of diet, an intraperitoneal glucose tolerance test (IPGTT) was performed to evaluate glucose homeostasis. Animals were fasted for 6 h, with free access to water during the entire experiment. Mice were weighted and the extremity of the tail was incised to obtain a small drop of blood, which was placed on the test strip of the blood glucometer (Bayer, ContourXT). The value obtained corresponds to the fasting blood glucose level. Then, a bolus of glucose diluted in 0.9% NaCl (1 g/kg) was injected in the intraperitoneal cavity and glycemia was measured again at 15, 30, 60, 90, and 120 min after the injection of glucose. Four days after IPGTT, mice were anesthetized, and the heart was rapidly collected and washed in cold phosphate-buffered saline (PBS) before freeze clamping.

Primary Culture of Adult Rat Cardiomyocytes

Adult rat cardiomyocytes were isolated as previously described (34). Hearts from anesthetized 250-g male Wistar rats were excised and perfused retrogradely via the aorta. After 10 min of perfusion with Ca^{2+}-free Krebs-Henseleit buffer [5 mM glucose, 2 mM pyruvate, 10 mM HEPES (pH 7.4) and 150 mM NaCl], hearts were digested by adding 0.2 mM Ca^{2+}, 1 mg/mL type 2 collagenase (Worthington), and 0.4% (wt/vol) fatty acid-free bovine serum albumin (BSA). Hearts were then removed from the perfusion apparatus and mechanically disrupted using scissors. Ca^{2+} was progressively increased in the medium to reach a final concentration of 1 mM. Cardiomyocytes were purified by sedimentation and distributed equally in laminin-coated dishes after resuspension in medium 199 [supplemented with 2 mM carnitine, 5 mM creatine, 5 mM taurine, 10^{-10} M T3, 0.2% (wt/vol) fatty acid-free BSA, and antibiotics]. Cardiomyocytes were treated according to the figure legends. Insulin resistance was induced by a 24-h hyperinsulinemic pretreatment (100 nM insulin) as described (34).

Tissue and Cell Lysis

For heart tissue, proteins were extracted with Ultra-turrax in RIPA lysis buffer [50 mM Tris (pH 8), 150 mM NaCl, 5 mM EDTA, 1% (vol/vol) NP-40, 0.5% (wt/vol) sodium deoxycholate, 0.1% (wt/vol) SDS, 0.5 mM PMSF, 1 mM benzamidine-HCl, 1 μg/mL leupeptine, 1 μg/mL pepstatin A, 1 mM DTT, 1 mM Na_3VO_4, 10 μM EX527, and 1 μM TSA). Lysates were then centrifuged (3,500 *g*, 10 min, 4°C), and protein content was determined with bicinchoninic acid assay according to the manufacturer instructions (Thermo Scientific, No. 23235). Cultured cardiomyocytes were lysed in 50 mM Tris·HCl (pH 7.5), 1 mM EDTA, 1 mM EGTA, 0.27 M sucrose, 1% (vol/vol) Triton X-100, 20 mM glycerol-2-phosphate, 50 mM NaF, 5 mM $Na_4P_2O_7$, 0.5 mM PMSF, 1 mM benzamidine-HCl, 1 μg/mL

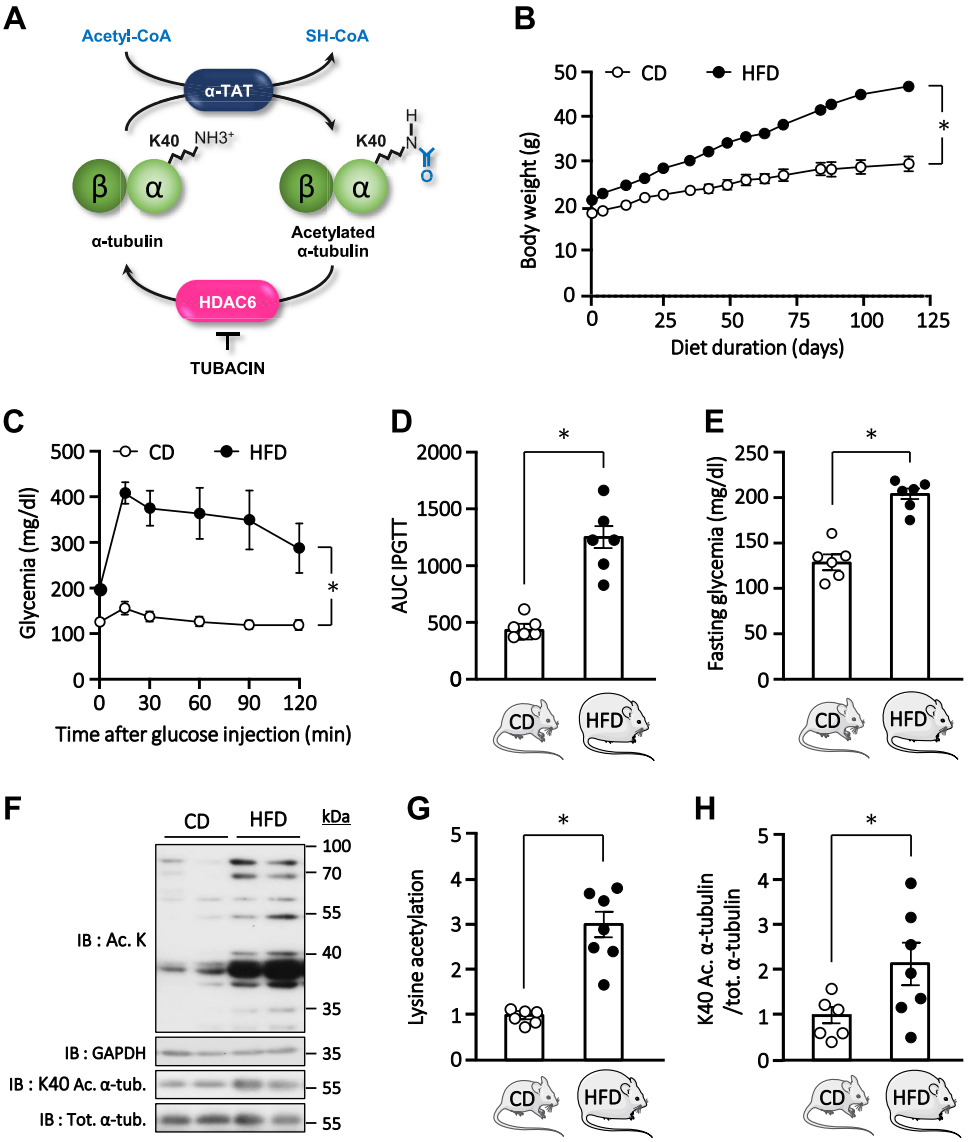

Figure 1. Global protein acetylation and α-tubulin K40 acetylation are increased in an HFD-mediated diabetic mouse model. *A*: schematic representation of physiological and pharmacological regulation of α-tubulin K40 acetylation. Characterization of HFD-induced diabetic mouse model with body weight evolution during 4 mo of diet (*B*), glycemia measurement during intraperitoneal glucose tolerance test (IPGTT) (*C*), quantification of the areas under the curve of IPGTT (*D*), and fasting glycemia (*E*) at 4 mo of diet. *F*: immunoblot analysis of global protein acetylation, K40 acetylated α-tubulin, and total α-tubulin with GAPDH as loading control in mouse hearts after 4 mo of CD or HFD and their respective quantification relative to CD (*G* and *H*); n = 6 to 7 animals/group. Values are expressed as means ± SE. Statistical analysis was performed via unpaired Student's t test (for *D*, *E*, *G*, and *H*) or two-way ANOVA (for *B* and *C*). *$P \leq 0.05$ relative to control group. Ac, acetylated; CD, chow diet; HFD, high-fat diet; IB, immunoblot; K, lysine; Tot, total; Tub, tubulin.

leupeptine, 1 μg/mL pepstatin A, 1 mM DTT, 1 mM Na_3VO_4, 10 μM EX527, and 1 μM TSA. Lysates were then centrifuged (3,500 *g*, 10 min, 4°C), and protein content was measured with Bradford assay.

Measurement of Glucose Uptake and Glycolysis

Glucose uptake and glycolysis were assessed by following the detritiation rate of [2-^{3}H]-glucose and [3-^{3}H]-glucose, respectively (34). Briefly, for the last 30 min of treatment, 0.2 μCi/mL of [2-^{3}H]-glucose or [3-^{3}H]-glucose was added to the cell culture medium. After acid precipitation of proteins, tritiated water accumulated from glucose detritiation was separated from tritiated glucose by borate-coupled column chromatography and measured with a scintillation counter as described (34).

Immunoblot Analysis

Tissue and cell lysates were used to study protein expression, phosphorylation, and acetylation levels by immunoblotting. The complete set of antibodies used in the present study can be found in the Supplemental Table S1 (see https://doi.org/10.6084/m9.figshare.17026496). Band intensity was quantified by ImageJ software and normalized with internal eukaryotic elongation factor 2 (eEF2) or glyceraldehyde-3-phosphate dehydrogenase (GAPDH). Quantification of phosphorylated or acetylated forms of proteins implied additional normalization relative to their respective total form. The original uncropped images of the blots presented in the figures can be found in Supplemental Fig. S9 (all Supplemental Figures are available at https://doi.org/10.6084/m9.figshare.17026436).

Evaluation of GLUT4 Translocation to the Plasma Membrane

The adenoviral construct expressing hemagglutinin (HA)-GLUT4-green fluorescent protein (GFP) was kindly provided by Dr. Corley Mastick (Department of Biochemistry and Molecular Biology, University of Nevada, Reno, NV) (35). Exogenous GLUT4 was tracked thanks to the fusion of GFP

at the GLUT4 carboxyl terminus. In addition, an HA epitope was inserted in the first exofacial loop of GLUT4, allowing the exclusive detection of GLUT4 inserted into the plasma membrane of nonpermeabilized cardiomyocytes. Primary cultured adult rat cardiomyocytes were plated on laminin-coated coverslips and were infected with HA-GLUT4-GFP adenovirus at a multiplicity of infection (MOI) of 10 for 48 h (36). After 10-min fixation with 4% (wt/vol) paraformaldehyde and 30 min blocking with 5% (wt/vol) BSA-PBS, non-permeabilized cells were incubated for 1 h with a primary antibody targeting HA epitope, followed by 1 h incubation with a secondary fluorescent antibody (see Supplemental Table S1 for antibody references). Red fluorescence coming from Alexa Fluor and intrinsic green fluorescence of GFP were visualized under a Zeiss Imager.Z1 microscope equipped with an ApoTome device. Red fluorescence (HA-staining) corresponding to membrane GLUT4 was quantified relative to GFP (total exogenous GLUT4) by ImageJ software.

Adenoviral Cloning of mCherry α-Tubulin K40A

An adenoviral particle expressing a K40A mutated form of α-tubulin fused to mCherry (mCherry α-tubulin K40A) was generated using the Adeasy system (Agilent Technologies). The pcDNA3 plasmid containing the cDNA coding for mCherry α-tubulin protein was kindly provided by Roger Tsien's laboratory (37) and the mutagenesis of K40 into an alanine residue was performed in Frédéric Saudou's laboratory (28). Briefly, mCherry α-tubulin K40A cDNA was amplified from the pcDNA3 plasmid before being inserted in the Adeasy pShuttle-CMV vector. Linearized pShuttle-mCherry α-tubulin K40A was transformed into BJ5183 bacteria, which contained the pAdEasy vector, allowing recombination. After amplification and linearization, the viral vector was transfected into HEK293T cells for adenoviral amplification. Amplified adenoviruses were purified on cesium chloride gradient as described (38).

Immunofluorescent Staining of Total α-Tubulin and K40 Acetylated α-Tubulin

Primary cultured cardiomyocytes were plated on laminin-coated coverslips. At the end of the experiment, cells were fixed with 4% (wt/vol) paraformaldehyde for 10 min at room temperature. Blocking and permeabilization were achieved with a 30 min incubation with a 2% (wt/vol) BSA-PBS solution containing 0.2% (vol/vol) Triton X-100. Cells were incubated with a primary antibody targeting total α-tubulin or K40 acetylated α-tubulin for 1 h and then with a secondary antibody coupled to an Alexa Fluor (references in Supplemental Table S1). Mutated α-tubulin K40A was visualized thanks to the fused mCherry domain. Pictures were taken with LSM800 confocal microscope.

Statistics

Results are expressed as means ± SE. Statistical significance was calculated with GraphPad Prism 9 using unpaired Student's *t* test when comparing two conditions or by one- or two-way analysis of variance (ANOVA) for multiple comparisons with Dunnett's or Sidak's post hoc test, respectively. A *P* value of 0.05 or less was considered statistically significant.

RESULTS

α-Tubulin K40 Acetylation Level Is Increased in a Diet-Induced Mouse Model of Diabetes

We first evaluated the impact of diet-induced diabetes on cardiac α-tubulin K40 acetylation level. Mice were fed for 4 mo with HFD or regular chow diet (CD) and a significant weight gain was observed in mice under HFD (Fig. 1*B*). Induction of diabetes in the HFD model was validated by showing a glucose intolerance (Fig. 1, *C* and *D*) and an increase in fasting glycemia (Fig. 1*E*) compared with control animals. As previously described in similar diet-induced diabetic models (39), HFD treatment promoted an increase in global cardiac protein acetylation levels, as followed by immunoblot using an anti-pan-acetyl lysine antibody (Fig. 1, *F* and *G*). Analogously, the specific α-tubulin K40 acetylation level was also found to be increased in the heart of HFD-fed mice (Fig. 1, *F* and *H*), suggesting that cardiac α-tubulin may be one of the proteins sensing excessive substrates. HFD leads to metabolic overfueling, resulting in an increase in acetyl-CoA production. As the substrate of acetyltransferases, this increase in acetyl-CoA production looks sufficient to explain the rise in protein acetylation. Nevertheless, we also studied the expression of SIRT1 (the main cytosolic deacetylase), HDAC6 and SIRT2 (assumed deacetylases of α-tubulin K40). As shown in Supplemental Fig. S1, HDAC6 and SIRT2 expression were slightly increased in the heart of HFD mice, whereas we did not observe any change in SIRT1 expression. The increase in HDAC6 and SIRT2 expression may reflect the effort of the cells to counteract the global increase in protein acetylation.

Increase in α-Tubulin K40 Acetylation Level Inhibits Glucose Transport and Glycolytic Flux in Adult Cardiomyocytes

To assess the role of α-tubulin K40 acetylation level on glucose transport, we incubated primary cultured adult rat cardiomyocytes with tubacin, a well-described selective HDAC6 inhibitor, the deacetylase responsible for tubulin deacetylation (Fig. 1*A*) (40). HDAC6 inhibition by increasing concentrations of tubacin (up to 30 μM, 5 h) progressively enhanced α-tubulin K40 acetylation level (being significant from 1 μM and reaching a plateau around 10 μM) without affecting total α-tubulin protein level (Fig. 2, *A* and *B*). In line with previous studies showing high specificity of tubacin toward α-tubulin acetylation (40), the global protein acetylation profile showed an increased signal for a single band located around 55 kDa that likely corresponds to tubulin molecular weight (Fig. 2*A*). According to these results, a dose of 10 μM tubacin was chosen to study the impact of an increase in α-tubulin K40 acetylation on basal glucose uptake and insulin-induced glucose uptake after 3 nM insulin stimulation, corresponding to the insulin half-maximal effective concentration (EC_{50}). Tubacin-mediated elevation of α-tubulin K40 acetylation was associated with a 40% reduction of both basal and insulin-induced glucose uptake (Fig. 2, *C* and *E*). Remarkably, relative insulin stimulation remained unchanged in both groups, with a respective 5.1- and 6.6-fold increase in the absence or presence of tubacin, suggesting that insulin

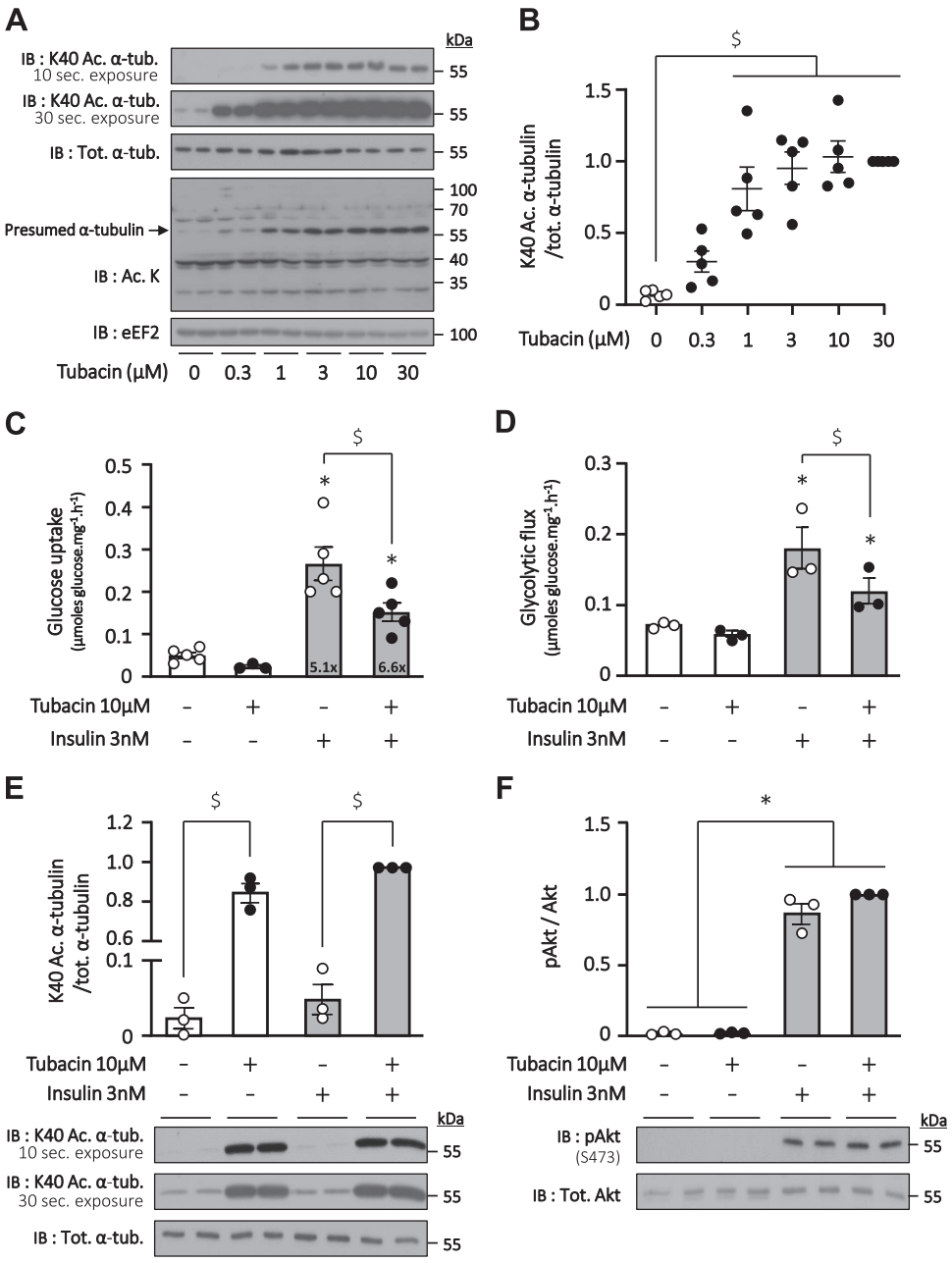

Figure 2. HDAC6 pharmacological inhibition increases α-tubulin K40 acetylation and inhibits glucose transport and glycolysis in cardiomyocytes. *A*: immunoblot analysis of α-tubulin K40 acetylation, total α-tubulin, global lysine acetylation, and eEF2 as loading control from primary cultured adult rat cardiomyocytes treated with increasing concentrations of tubacin (0 to 30 μM, 5 h). *B*: α-tubulin K40 acetylation quantification relative to 30 μM tubacin-treated cells (n = 5 biological replicates). Glucose uptake (*C*) and glycolytic flux (*D*) measured in cardiomyocytes treated or not with 10 μM tubacin for 5 h in presence or absence of 3 nM insulin for the last 30 min. Numbers in histogram bars indicate the relative increase in glucose uptake (*C*) in response to insulin compared to their respective controls (n = 3–5 biological replicates). *E* and *F*: immunoblot analysis of α-tubulin K40 acetylation, total α-tubulin, and PKB/Akt phosphorylation after a 5-h incubation with or without 10 μM tubacin and in presence or absence of 3 nM insulin for the last 30 min and their quantification compared with tubacin-treated cells with insulin (n = 3 biological replicates). Values are expressed as means ± SE. Statistical analysis was carried out by one-way (*B*) or two-way (*C*–*F*) ANOVA. \$$P \leq 0.05$ relative to respective tubacin-untreated cells; *$P \leq 0.05$ relative to respective insulin-unstimulated cells. Ac, acetylated; IB, immunoblot; K, lysine; Tot, total; Tub, tubulin.

response per se was not impacted by HDAC6 inhibition. Interestingly, insulin-stimulated glycolytic flux was also impaired by tubacin treatment, suggesting that reduction of glucose transport is reflected on its downstream catabolism (Fig. 2*D*). However, decrease in glucose uptake and glycolysis does not seem to be caused by an inhibition of the insulin signaling pathway as insulin-mediated phosphorylation of PKB/Akt, the main effector of insulin pathway, remained unaffected by tubacin treatment (Fig. 2*F*). This is also strengthened by the fact that tubacin was able to further inhibit insulin-stimulated glucose transport in cells presenting an insulin resistance (Supplemental Fig. S2). It is interesting to note that the inhibitory effect of tubacin-mediated α-tubulin K40 acetylation on glucose transport was not due to an alteration of the microtubule network, as its structure was similar in control and tubacin-treated cardiomyocytes (Supplemental Fig. S3). Taken together, these results highly suggest that an increase in α-tubulin acetylation on K40 negatively regulates glucose transport in cardiomyocytes, without any impact on insulin signaling pathway and microtubule integrity.

Increased α-Tubulin K40 Acetylation Level Inhibits GLUT4 Translocation to the Plasma Membrane

We then evaluated tubacin effect on GLUT4 translocation from vesicular pools to the plasma membrane along the microtubule network. For this purpose, cardiomyocytes were infected with an adenoviral construct coding for a chimeric protein where a hemagglutinin-tagged GLUT4 was fused to the green fluorescent protein (HA-GLUT4-GFP). This construct has already been successfully used for similar evaluation (17, 35). Detection of GFP intrinsic fluorescence (green) allows the monitoring of the total expressed GLUT4

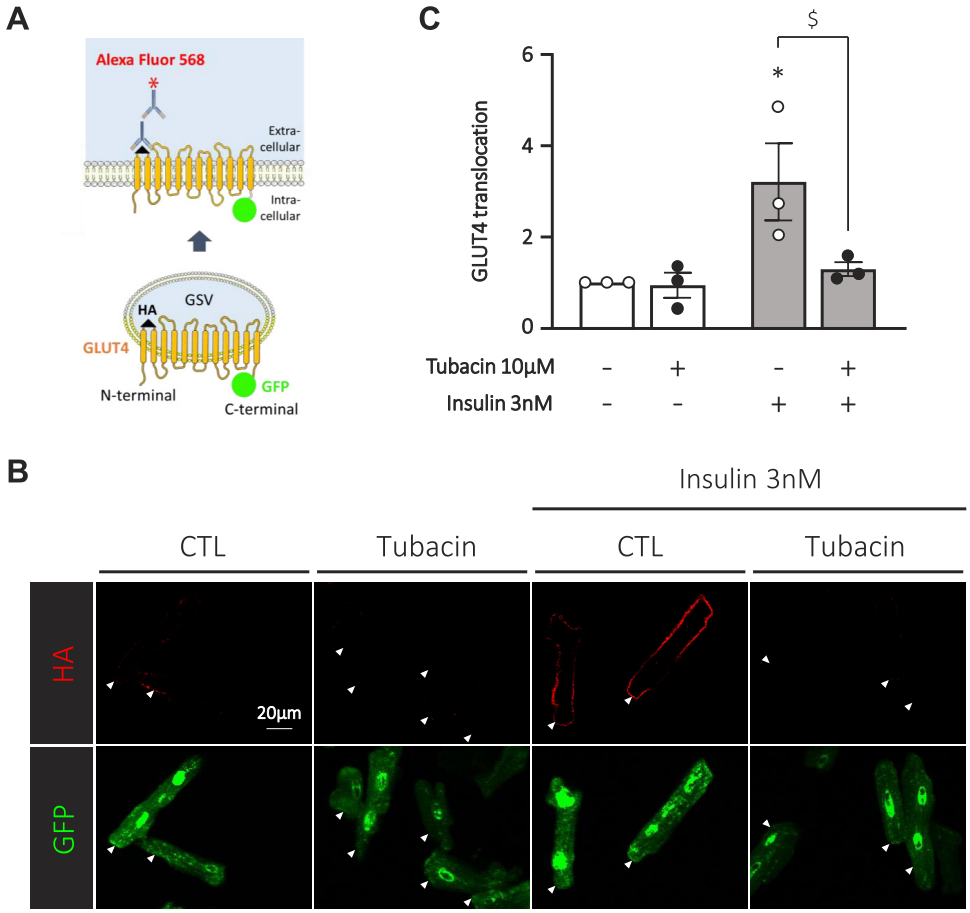

Figure 3. Tubacin inhibits GLUT4 translocation to the plasma membrane. *A*: schematic representation of fusion protein HA-GLUT4-GFP. *B*: immunolabeling of GLUT4 translocation in primary cultured adult rat cardiomyocytes infected 48 h with HA-GLUT4-GFP pretreated 5 h with or without 10 μM tubacin and treated or not with 3 nM insulin for the last 30 min. *C*: GLUT4 translocation quantification reflected by red (HA) on green (GFP) ratios of pixel intensity quantified by Axiovision/ImageJ and expressed compared with tubacin- and insulin-untreated cells. White arrows indicate cell plasmatic membrane localization. Values are expressed as means ± SE of 3 independent experiments relative to the control group. Statistical analysis was realized using two-way ANOVA. $*P \leq 0.05$ relative to respective insulin-unstimulated cells; $\$P \leq 0.05$ relative to respective tubacin-untreated cells. GFP, green fluorescent protein; HA, hemagglutinin.

pool, whereas immunofluorescent staining (red) of the HA tag, located in an extracellular loop of GLUT4, specifically reflects GLUT4 inserted into the plasma membrane of nonpermeabilized cardiomyocytes (Fig. 3*A*). As previously shown (17), insulin stimulation of infected cardiomyocytes promoted GLUT4 translocation to the plasma membrane (Fig. 3, *B* and *C*). More interestingly, a 5 h pretreatment with 10 μM tubacin abolished such insulin-induced GLUT4 translocation. These data strongly suggest that an increase in α-tubulin K40 acetylation reduces the presence of GLUT4 at the plasma membrane upon insulin stimulation, therefore offering a possible explanation for tubacin-mediated decrease in glucose uptake.

Overexpression of a Nonacetylable Form of α-Tubulin Enhances Basal and Insulin-Stimulated Glucose Uptake

We also investigated the effect of a decrease in α-tubulin K40 acetylation level on cardiac glucose transport by overexpressing a nonacetylable form of α-tubulin, where K40 is replaced by an alanine residue (K40A) (28, 41). This mutated α-tubulin was fused to the mCherry domain (mCherry α-tubulin K40A) to evaluate its cellular localization (37). Primary cultured cardiomyocytes were infected with an adenoviral construct coding for the chimeric protein 48 h before any treatment to allow transgene expression and protein integration into the microtubule system. We used an adenovirus coding for the β-galactosidase as control because the corresponding mCherry α-tubulin K40K was not acetylated when overexpressed in the timeframe used, so acting similarly to the mutated α-tubulin K40A (data not shown). We first checked the integration of mCherry α-tubulin K40A, and Fig. 4*A* clearly shows a similar and typical microtubule network organization when comparing the endogenous α-tubulin in control cardiomyocytes (infected with control adenovirus coding for β-galactosidase and immunolabeled in red using an anti-α-tubulin antibody) with the overexpressed mCherry α-tubulin K40A in cardiomyocytes infected with the mutant construct (following red mCherry intrinsic fluorescence). In comparison, treating control cardiomyocytes with nocodazole, a well-known inhibitor of microtubule polymerization, resulted in a completely different organization corresponding to a disorganized tubulin network, which is accompanied by impaired glucose uptake (Supplemental Fig. S4). This highly suggests that the mutant protein correctly incorporates into microtubules. Increasing expression of mCherry α-tubulin K40A was then detected by Western blot at the expected molecular weight of 85 kDa (55 kDa + 30 kDa for α-tubulin and mCherry, respectively), whereas endogenous α-tubulin was detected around its predicted weight of 55 kDa (Fig. 4*B*). As expected, mCherry α-tubulin K40A was not detected by the anti-K40 acetylated α-tubulin antibody (Fig. 4*B*). More interestingly, such overexpression progressively reduced endogenous α-tubulin K40 acetylation level as observed by Western blot (Fig. 4*B*), showing the capacity of this construct to act as a dominant negative, as described

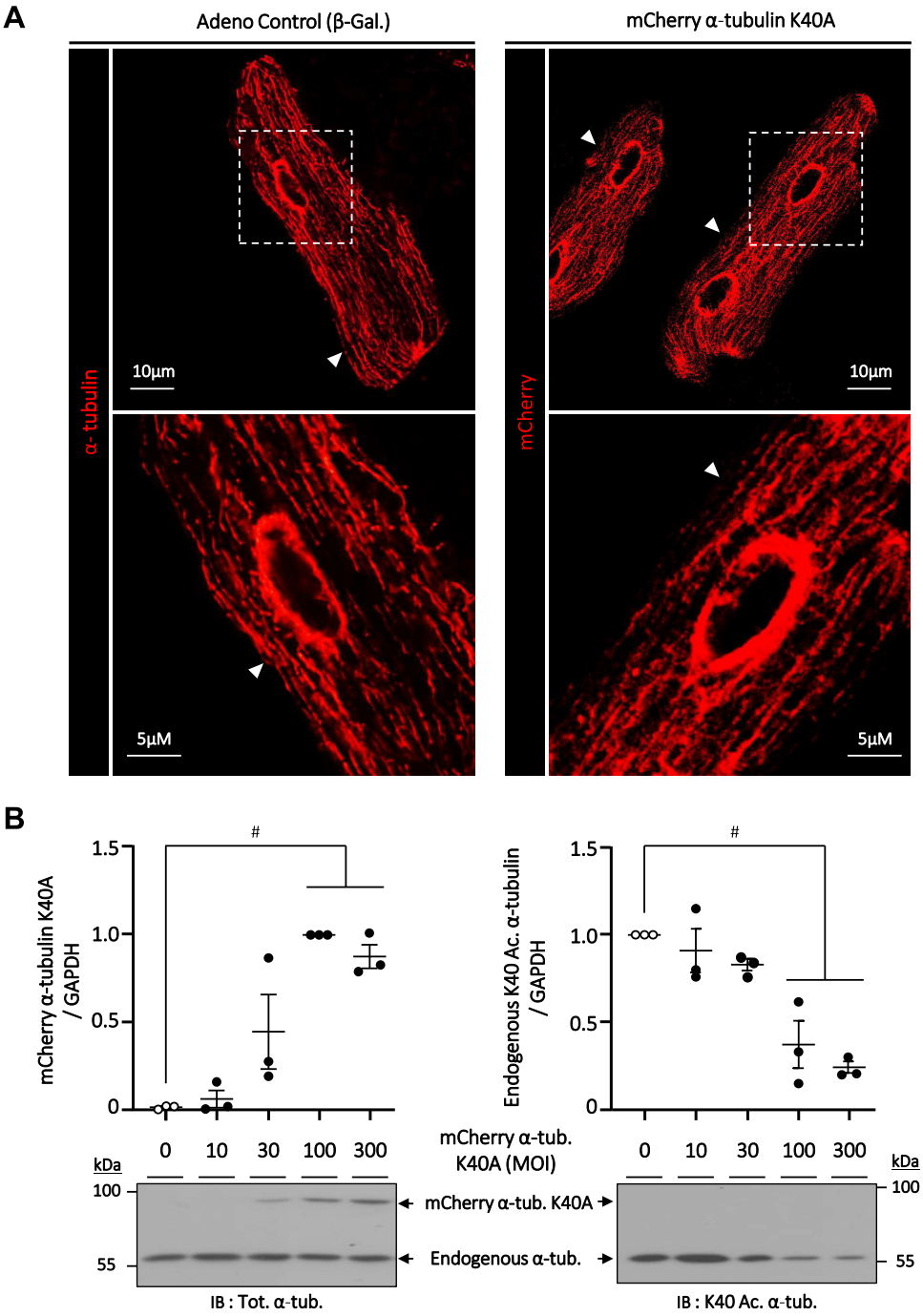

Figure 4. Overexpressing a nonacetylable α-tubulin (mCherry α-tubulin K40A) integrates microtubule network and decreases endogenous α-tubulin acetylation level on K40. *A*: microtubule network organization: immunolabeled endogenous α-tubulin in primary cultured adult rat cardiomyocytes infected with β-galactosidase-expressing adenovirus (*left*) and mCherry α-tubulin K40A in primary cultured adult rat cardiomyocytes infected with adenoviral particles encoding for mCherry α-tubulin K40A (*right*). *B*: immunoblotting in cardiomyocytes infected with increasing doses of adenovirus coding for mCherry α-tubulin K40A (0 to 300 MOI): endogenous α-tubulin immunoblotting (around 55 kDa) or immunoblotting and quantification (relative to 100 MOI infection) of mCherry α-tubulin K40A (~85 kDa) (*left*) and K40 acetylation immunoblotting of mCherry α-tubulin K40A and endogenous α-tubulin and its relative quantification to control cardiomyocytes (*right*). White arrows indicate cell plasmatic membrane localization. Values represent means ± SE of 3 independent experiments. One-way ANOVA was performed for statistical analysis. #$P \leq 0.05$ relative to cells infected with control adenovirus. Ac, acetylated; β-Gal, β-galactosidase; IB, immunoblot; Tot, total; Tub, tubulin.

previously (28). Similarly, the increase in endogenous α-tubulin K40 acetylation induced by tubacin was reduced in the presence of mCherry α-tubulin K40A (Supplemental Fig. S5). An anti-pan-acetylated lysine Western blot confirmed the decrease in acetylation levels of the presumed endogenous α-tubulin band around 55 kDa. Of particular interest, this antibody did not detect any band corresponding to the mCherry α-tubulin K40A (around 85 kDa), confirming tubacin specificity toward the exclusive acetylation of α-tubulin (Supplemental Fig. S5).

We then evaluated the effect of mCherry α-tubulin K40A on basal and insulin-stimulated glucose uptake. Decrease in α-tubulin K40 acetylation level promoted by this dominant form was accompanied by a significant increase in basal glucose uptake (Fig. 5*A*). The insulin dose-response curve next gave a classical sigmoidal shape in both control cells and cells overexpressing mCherry α-tubulin K40A with stimulation of glucose uptake starting at around 1 nM and reaching a maximum at 10 nM (Fig. 5*B*). PKB/Akt phosphorylation level followed a similar profile (Fig. 5*C*). More interestingly, the expression of the nonacetylable α-tubulin mutant sensitized cardiomyocytes to insulin, with enhanced glucose transport at every insulin concentration used. Downstream glucose entry into the cells, both basal and insulin-stimulated glycolytic

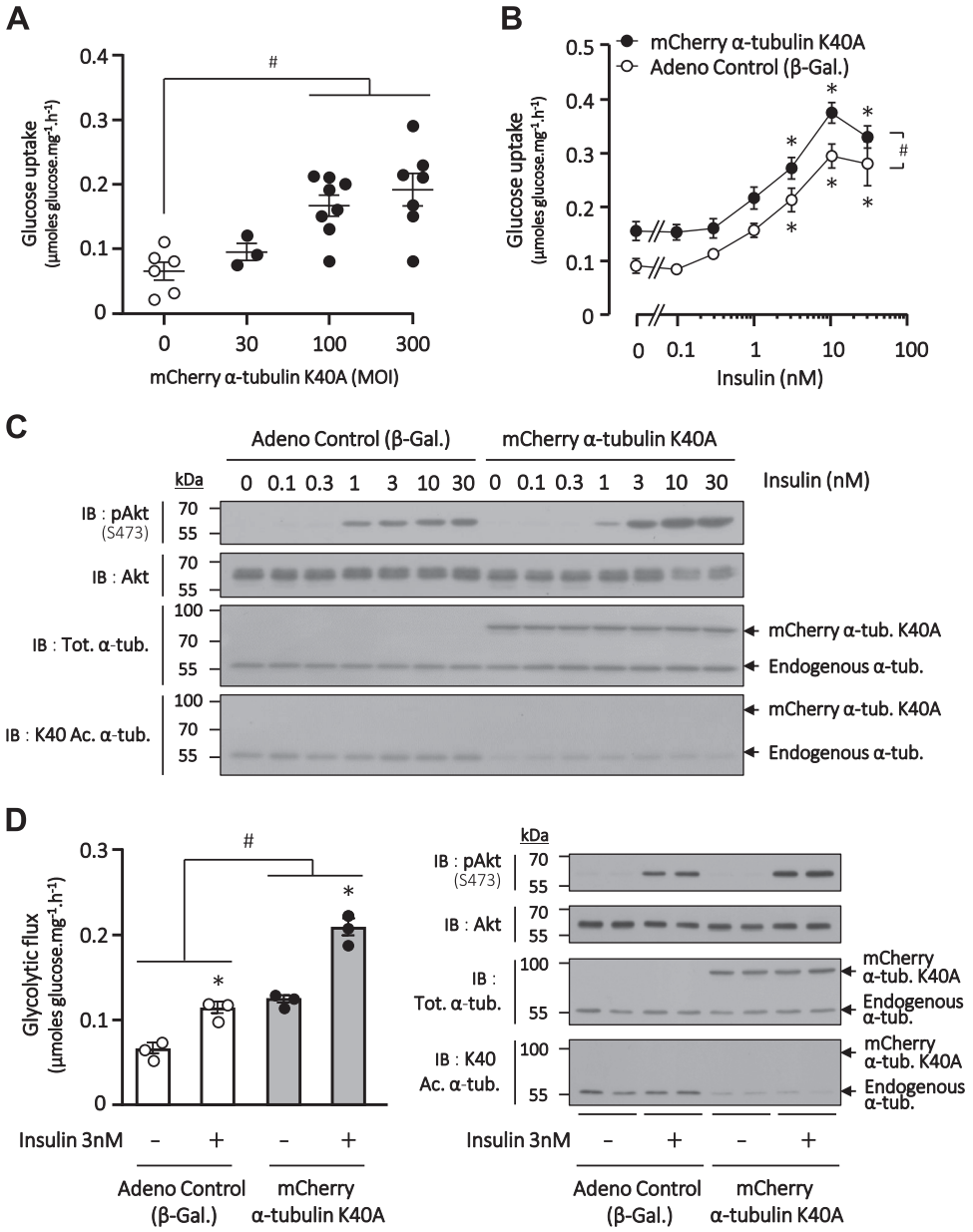

Figure 5. Decreased α-tubulin K40 acetylation promotes glucose uptake and glycolysis in insulin-sensitive cardiomyocytes. *A*: glucose uptake measurement in primary cultured adult rat cardiomyocytes infected for 48 h with control adenovirus coding for β-galactosidase or with increasing doses of adenovirus coding for mCherry α-tubulin K40A (up to 300 MOI) (n = 3–8 biological replicates). Glucose uptake (*B*) and immunoblot analysis of phosphorylated and total PKB/Akt, K40 acetylated, and total α-tubulin (*C*) in cardiomyocytes overexpressing mCherry α-tubulin K40A (100 MOI) or β-galactosidase (adeno control) and treated with increasing concentrations of insulin (0 to 30 nM) for the last 30 min (n = 3 to 4 biological replicates). *D*: glycolytic flux measured in cardiomyocytes infected with adeno control (β-galactosidase) or mCherry α-tubulin K40A for 48 h and treated or not with insulin 3 nM for the last 30 min (*left*) and their immunoblot analysis of phosphorylated and total PKB/Akt, K40 acetylated and total α-tubulin (*right*) (n = 3 biological replicates). Quantification of those immunoblots can be found in Supplemental Fig. S6. Values are expressed as means ± SE. Statistical analysis was carried out via one-way (*A*) or two-way (*B* and *D*) ANOVA. #$P \leq 0.05$ relative to cells infected with control adenovirus; *$P \leq 0.05$ relative to respective insulin-unstimulated cells. Ac, acetylated; β-Gal, β-galactosidase; IB, immunoblot; Tot, total; Tub, tubulin.

fluxes were similarly increased by overexpression of the nonacetylable α-tubulin K40A mutant, independently of the insulin signaling pathway (Fig. 5*D* and Supplemental Fig. S6). To definitively rule out the role of insulin signaling, we also tested the effect of the α-tubulin K40A mutant on the stimulation of glucose uptake by another pathway, namely, the AMP-activated protein kinase (AMPK). Accordingly, the stimulation of glucose transport in response to the AMPK activator oligomycin (1 µM, 1 h) was significantly enhanced by the K40A mutant overexpression (Supplemental Fig. S7). Together, these data support the fact that decreasing acetylation level of α-tubulin on K40 increases both glucose transport and glycolysis.

mCherry α-Tubulin K40A Overexpression Enhances Glucose Uptake in Insulin-Resistant Cardiomyocytes

Because insulin signaling pathway does not seem to be involved in the modulation of glucose uptake by α-tubulin K40 acetylation, we investigated whether mCherry α-tubulin K40A overexpression could rescue insulin-stimulated glucose uptake in insulin-resistant cardiomyocytes that exhibit impaired insulin signaling and glucose transport. For that purpose, we used primary cultured cardiomyocytes where acute insulin resistance was promoted by a 1-day preexposure to a supraphysiological concentration of insulin (34). As demonstrated before (34), such exposition nicely recapitulated an insulin-resistant state, characterized by the loss of insulin response in terms of both signaling (PKB/Akt phosphorylation) and glucose uptake (Fig. 6 and Supplemental Fig. S8) that are independent of α-tubulin K40 acetylation level increase. According to our previous experiments, overexpression of mCherry α-tubulin K40A reduced α-tubulin K40 acetylation level and increased both basal and insulin-stimulated glucose uptake in insulin-sensitive cells (Fig. 6). Although it similarly decreased α-tubulin K40 acetylation in

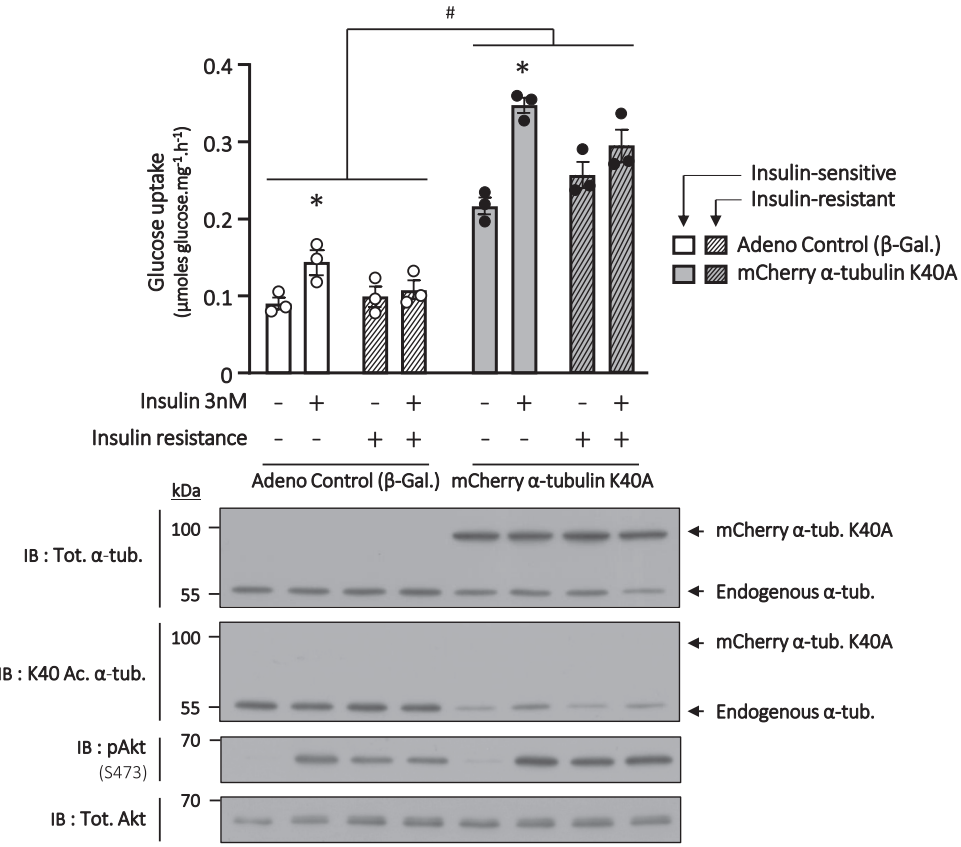

Figure 6. Decreased α-tubulin K40 acetylation promotes glucose uptake in insulin-resistant cardiomyocytes. Glucose uptake and immunoblotting of total α-tubulin and α-tubulin K40 acetylation or phosphorylated and total PKB/Akt in primary cultured adult rat cardiomyocytes infected with control β-galactosidase adenovirus or with mCherry α-tubulin K40A adenovirus (100 MOI) for 24 h before inducing or not insulin resistance through a 24-h exposition to 100 nM insulin. Cardiomyocytes were then treated or not with 3 nM insulin for the last 30 min. Quantification of those immunoblots is available in Supplemental Fig. S8. Values are expressed as means ± SE of 3 independent experiments. Effect of K40A overexpression has been analyzed by two-way ANOVA on the full data set, whereas insulin effect has been analyzed by two-way ANOVA in each subgroup (adeno control (β-Gal.) and mCherry α-tubulin K40A adenoviruses). #$P \leq 0.05$ relative to cells infected with adeno control (β-Gal); *$P \leq 0.05$ relative to insulin-unstimulated cells. Ac, acetylated; β-Gal, β-galactosidase; IB, immunoblot; Tot, total; Tub, tubulin.

insulin-resistant cells (Fig. 6 and Supplemental Fig. S8), it did not restore their capacity to respond to insulin. Nevertheless, it led to a global increase in glucose uptake to reach levels higher than those observed in insulin-sensitive cardiomyocytes (Fig. 6). From all these experiments, we can conclude that reducing α-tubulin K40 acetylation level improves global glucose uptake in cardiomyocytes and that such an intervention can bypass insulin resistance to increase glucose uptake.

DISCUSSION

We previously showed that an excess of nutrients rapidly increases cardiac protein acetylation level, resulting in the inhibition of insulin-stimulated glucose uptake via a defect in GLUT4 translocation (17). Indeed, the catabolism of ATP-providing nutrients mainly converges to the production of acetyl-CoA that not only feeds the Krebs cycle but also fuels acetyltransferases that promote a global increase in protein acetylation under overfueling conditions (42). However, the precise molecular mechanisms by which protein acetylation reduces glucose uptake and the identity of the acetylated proteins involved in this process remain undetermined. The results presented here demonstrate that among many proteins, acetylation of α-tubulin on K40 is an important piece of the puzzle. To summarize, we showed that *1*) cardiac α-tubulin K40 acetylation level is increased in a chronic context of diabetes resulting from HFD; *2*) increasing α-tubulin K40 acetylation by the specific HDAC6 inhibitor, tubacin, reduces glucose entry and glycolysis in cardiomyocytes; and, conversely, *3*) reducing α-tubulin K40 acetylation level, by expressing a nonacetylable form of α-tubulin, boosts glucose uptake and glycolysis in both insulin-sensitive and insulin-resistant cardiomyocytes. Altogether, this work proposes that an increase in α-tubulin K40 acetylation is an important event, but probably not the only one, that impairs GLUT4 trafficking and subsequent glucose uptake. Therefore, reducing α-tubulin K40 acetylation level may be an interesting lead to improve glucose uptake in pathological contexts, for example, as an additive mean to restore glucose homeostasis in patients with diabetes.

It is interesting to notice that modulating α-tubulin K40 acetylation affects both basal and insulin-induced glucose uptake without altering the amplitude of insulin signaling and response. One explanation could lie in the alteration of the dynamic retention model of GLUT4, which proposes that the transporter undergoes continuous exocytosis/endocytosis cycles controlling its presence at the plasma membrane, even in basal state, and that insulin enhances its exocytosis rate (43). It is therefore tempting to speculate that α-tubulin acetylation impacts trafficking along microtubules, which could actively participate in the regulation of this dynamic model. This hypothesis is reinforced by the fact that tubacin-mediated α-tubulin K40 acetylation impairs insulin stimulation of GSVs translocation to the plasma membrane. One could therefore postulate that α-tubulin K40 acetylation either impairs GLUT4 exocytosis, stimulates its endocytosis, or reduces the pool of GLUT4 vesicles available for translocation. This hypothesis is supported by the fact that AMPK is described to regulate these three events (44).

Converging evidence in literature indicates that K40-acetylated α-tubulin rather favors recruitment to the microtubule

network of motor proteins such as dynein or kinesin, suggesting a global acceleration of vesicular trafficking (25, 26, 28). To fully address this question, it will be highly valuable to assess more deeply how intracellular GLUT4 trafficking is affected by α-tubulin K40 acetylation. Beyond GLUT4 trafficking, α-tubulin K40 acetylation may also affect trafficking of other important cardiac transporters located in vesicles such as the fatty acids transporter CD36. A better comprehension of these events could increase our general knowledge of pathologies, such as diabetes, in which acetylation is globally increased.

One may wonder whether tubacin-mediated glucose uptake inhibition could result from nonspecific effects of tubacin. Several arguments may nevertheless reduce the possibility of any major tubulin-independent action of tubacin. First, Haggarty et al. (40) deeply characterized the inhibitor and showed that tubacin does not promote histone acetylation or gene expression, ruling out unspecific effects of tubacin on other members of HDAC family. Therefore, tubacin can be considered as specific, if not even more, as genetically deleting HDAC6 that would inevitably affect all HDAC6 targets. Accordingly, we showed that tubacin increases the intensity of a unique band corresponding to α-tubulin molecular weight in the global protein acetylation Western blot. Finally, the decrease in α-tubulin K40 acetylation resulting from mCherry α-tubulin K40A expression largely hinders tubacin inhibitory effects on glucose uptake.

We can also question the importance of α-tubulin K40 acetylation in the decrease in glucose uptake under insulin-resistant situations. Indeed, α-tubulin K40 acetylation was not modified in our acute cellular model of insulin resistance, suggesting that acetylation of α-tubulin K40 may not be part of the initial defect causing the loss of insulin-stimulated glucose transport in cardiomyocytes. However, α-tubulin K40 acetylation is clearly exacerbated in our chronic in vivo diabetic model. This observation suggests that α-tubulin K40 acetylation may contribute to the development or may sustain the defect in insulin-stimulated glucose uptake at more advanced diabetes stages. Therefore, α-tubulin K40 acetylation represents an attractive target for stimulating glucose uptake in chronic pathologies characterized by insulin resistance. Accordingly, we expressed a nonacetylable mutant form of α-tubulin in our insulin-resistant cellular model with the idea of challenging the beneficial effect of a reduction of α-tubulin K40 acetylation levels. We showed that this mutant promotes a general improvement in glucose transport. However, it does not strictly reinstate insulin response. In other words, α-tubulin K40 acetylation reduction allows bypassing the loss of insulin signaling by promoting an insulin-independent increase in glucose uptake. Assuming that α-tubulin acetylation is similarly coupled to glucose uptake in skeletal muscle, we can also postulate that α-tubulin K40 acetylation may therefore constitute a promising candidate for pharmacological intervention to normalize overall glycemia in patient with diabetes in complement to existing medication.

Novelty and Limitations of The Study

It is the first time that α-tubulin K40 acetylation is shown to directly control glucose metabolism by inhibiting GLUT4 translocation. In addition to previously described roles of protein acetylation in the control of cardiac metabolism (42), it could contribute to the cardiac metabolic inflexibility and the establishment of diabetic cardiomyopathy. Future experimentation will aim to identify the underlying mechanisms involved and the other actors regulating this complex event, directly or indirectly. In line, it will be highly valuable to assess the role of α-tubulin acetylation in an in vivo model, and without overexpression, to complete our current results with cardiac function measurements.

SUPPLEMENTAL DATA

Supplemental Table S1: https://doi.org/10.6084/m9.figshare.17026496.

Supplemental Figs. S1–S9: https://doi.org/10.6084/m9.figshare.17026436.

ACKNOWLEDGMENTS

We thank P. Morue for work on tubacin experiments and Drs. F. Saudou and R. Y. Tsien for sharing mCherry α-tubulin and mCherry α-tubulin K40A cDNA materials.

GRANTS

This work was supported by grants from the Fonds National de la Recherche Scientifique (FNRS, Belgium) and Action de Recherche Concertée (Wallonia-Brussels Federation) and unrestricted grants from AstraZeneca. S. H. is FNRS Senior Research Associate.

DISCLOSURES

No conflicts of interest, financial or otherwise, are declared by the authors.

AUTHOR CONTRIBUTIONS

E.R., M.D.L., N.F., A.G., C.Bo., C.P., S.H., C.Be., L.Bu., and L.Be. conceived and designed research; E.R., M.D.L., N.F., A.G., and L.Bu. performed experiments; E.R., M.D.L., N.F., A.G., C.Bo., S.H., C.Be., L.Bu., and L.Be. analyzed data; E.R., M.D.L., N.F., A.G., C.Bo., C.P., S.H., C.Be., L.Bu., and L.Be. interpreted results of experiments; E.R., M.D.L., N.F., A.G., L.Bu., and L.Be. prepared figures; E.R., M.D.L., L.Bu., and L.Be. drafted manuscript; E.R., M.D.L., N.F., A.G., C.Bo., C.P., S.H., C.Be., L.Bu., and L.Be. edited and revised manuscript; E.R., M.D.L., N.F., A.G., C.Bo., C.P., S.H., C.Be., L.Bu., and L.Be. approved final version of manuscript.

REFERENCES

1. **Hue L**, **Taegtmeyer H.** The Randle cycle revisited: a new head for an old hat. *Am J Physiol Endocrinol Metab* 297: E578–E591, 2009. doi:10.1152/ajpendo.00093.2009.
2. **Randle PJ**, **Garland PB**, **Hales CN**, **Newsholme EA.** The glucose fatty-acid cycle. Its role in insulin sensitivity and the metabolic disturbances of diabetes mellitus. *Lancet* 1: 785–789, 1963. doi:10.1016/S0140-6736(63)91500-9.
3. **Belke DD**, **Larsen TS**, **Gibbs EM**, **Severson DL.** Altered metabolism causes cardiac dysfunction in perfused hearts from diabetic (db/db) mice. *Am J Physiol Endocrinol Metab* 279: E1104–E1113, 2000. doi:10.1152/ajpendo.2000.279.5.E1104.
4. **Wright JJ**, **Kim J**, **Buchanan J**, **Boudina S**, **Sena S**, **Bakirtzi K**, **Ilkun O**, **Theobald HA**, **Cooksey RC**, **Kandror KV**, **Abel ED.** Mechanisms for increased myocardial fatty acid utilization following short-term high-fat feeding. *Cardiovasc Res* 82: 351–360, 2009. doi:10.1093/cvr/cvp017.

5. **Ritchie RH**, **Abel ED.** Basic mechanisms of diabetic heart disease. *Circ Res* 126: 1501–1525, 2020. doi:10.1161/CIRCRESAHA.120.315913.
6. **Abel ED.** Glucose transport in the heart. *Front Biosci* 9: 201–215, 2004. doi:10.2741/1216.
7. **Bertrand L**, **Auquier J**, **Renguet E**, **Ange M**, **Cumps J**, **Horman S**, **Beauloye C.** Glucose transporters in cardiovascular system in health and disease. *Pflugers Arch* 472: 1385–1399, 2020. doi:10.1007/s00424-020-02444-8.
8. **Shao D**, **Tian R.** Glucose transporters in cardiac metabolism and hypertrophy. *Compr Physiol* 6: 331–351, 2015. doi:10.1002/cphy.c150016.
9. **Li DT**, **Habtemichael EN**, **Julca O**, **Sales CI**, **Westergaard XO**, **DeVries SG**, **Ruiz D**, **Sayal B**, **Bogan JS.** GLUT4 storage vesicles: specialized organelles for regulated trafficking. *Yale J Biol Med* 92: 453–470, 2019.
10. **Wang T**, **Wang J**, **Hu X**, **Huang X-J**, **Chen G-X.** Current understanding of glucose transporter 4 expression and functional mechanisms. *World J Biol Chem* 11: 76–98, 2020. doi:10.4331/wjbc.v11.i3.76.
11. **Bertrand L**, **Horman S**, **Beauloye C**, **Vanoverschelde J-L.** Insulin signalling in the heart. *Cardiovasc Res* 79: 238–248, 2008. doi:10.1093/cvr/cvn093.
12. **Jaldin-Fincati JR**, **Pavarotti M**, **Frendo-Cumbo S**, **Bilan PJ**, **Klip A.** Update on GLUT4 vesicle traffic: a cornerstone of insulin action. *Trends Endocrinol Metab* 28: 597–611, 2017. doi:10.1016/j.tem.2017.05.002.
13. **Klip A**, **McGraw TE**, **James DE.** Thirty sweet years of GLUT4. *J Biol Chem* 294: 11369–11381, 2019. doi:10.1074/jbc.REV119.008351.
14. **Huffman KM**, **Shah SH**, **Stevens RD**, **Bain JR**, **Muehlbauer M**, **Slentz CA**, **Tanner CJ**, **Kuchibhatla M**, **Houmard JA**, **Newgard CB**, **Kraus WE.** Relationships between circulating metabolic intermediates and insulin action in overweight to obese, inactive men and women. *Diabetes Care* 32: 1678–1683, 2009. doi:10.2337/dc08-2075.
15. **Newgard CB**, **An J**, **Bain JR**, **Muehlbauer MJ**, **Stevens RD**, **Lien LF**, **Haqq AM**, **Shah SH**, **Arlotto M**, **Slentz CA**, **Rochon J**, **Gallup D**, **Ilkayeva O**, **Wenner BR**, **Yancy WS Jr**, **Jr**,**Eisenson H**, **Musante G**, **Surwit RS**, **Millington DS**, **Butler MD**, **Svetkey LP.** A branched-chain amino acid-related metabolic signature that differentiates obese and lean humans and contributes to insulin resistance. *Cell Metab* 9: 311–326, 2009. [Erratum in *Cell Metab* 9:565-566, 2009]. doi:10.1016/j.cmet.2009.02.002.
16. **Alkhateeb H**, **Chabowski A**, **Glatz JFC**, **Luiken JFP**, **Bonen A.** Two phases of palmitate-induced insulin resistance in skeletal muscle: impaired GLUT4 translocation is followed by a reduced GLUT4 intrinsic activity. *Am J Physiol Endocrinol Metab* 293: E783–E793, 2007. doi:10.1152/ajpendo.00685.2006.
17. **Renguet E**, **Ginion A**, **Gélinas R**, **Bultot L**, **Auquier J**, **Robillard Frayne I**, **Daneault C**, **Vanoverschelde J-L**, **Des Rosiers C**, **Hue L**, **Horman S**, **Beauloye C**, **Bertrand L.** Metabolism and acetylation contribute to leucine-mediated inhibition of cardiac glucose uptake. *Am J Physiol Heart Circ Physiol* 313: H432–H445, 2017. doi:10.1152/ajpheart.00738.2016.
18. **Fletcher LM**, **Welsh GI**, **Oatey PB**, **Tavaré JM.** Role for the microtubule cytoskeleton in GLUT4 vesicle trafficking and in the regulation of insulin-stimulated glucose uptake. *Biochem J* 352: 267–276, 2000. [Erratum in *Biochem J* 353: 735, 2001]. doi:10.1042/bj3520267.
19. **Goodson HV**, **Jonasson EM.** Microtubules and microtubule-associated proteins. *Cold Spring Harb Perspect Biol* 10: a022608, 2018. doi:10.1101/cshperspect.a022608.
20. **L'Hernault SW**, **Rosenbaum JL.** Chlamydomonas alpha-tubulin is posttranslationally modified by acetylation on the epsilon-amino group of a lysine. *Biochemistry* 24: 473–478, 1985. doi:10.1021/bi00323a034.
21. **Sadoul K**, **Khochbin S.** The growing landscape of tubulin acetylation: lysine 40 and many more. *Biochem J* 473: 1859–1868, 2016. doi:10.1042/BCJ20160172.
22. **Kalebic N**, **Sorrentino S**, **Perlas E**, **Bolasco G**, **Martinez C**, **Heppenstall PA.** αTAT1 is the major α-tubulin acetyltransferase in mice. *Nat Commun* 4: 1962, 2013. doi:10.1038/ncomms2962.
23. **Kim G-W**, **Li L**, **Ghorbani M**, **You L**, **Yang X-J.** Mice lacking α-tubulin acetyltransferase 1 are viable but display α-tubulin acetylation deficiency and dentate gyrus distortion. *J Biol Chem* 288: 20334–20350, 2013. [Erratum in *J Biol Chem* 291: 25279, 2016]. doi:10.1074/jbc.M113.464792.
24. **Hubbert C**, **Guardiola A**, **Shao R**, **Kawaguchi Y**, **Ito A**, **Nixon A**, **Yoshida M**, **Wang X-F**, **Yao T-P.** HDAC6 is a microtubule-associated deacetylase. *Nature* 417: 455–458, 2002. doi:10.1038/417455a.
25. **Li L**, **Yang X-J.** Tubulin acetylation: responsible enzymes, biological functions and human diseases. *Cell Mol Life Sci* 72: 4237–4255, 2015.
26. **Balabanian L**, **Berger CL**, **Hendricks AG.** Acetylated microtubules are preferentially bundled leading to enhanced kinesin-1 motility. *Biophys J* 113: 1551–1560, 2017. doi:10.1016/j.bpj.2017.08.009.
27. **Cai D**, **McEwen DP**, **Martens JR**, **Meyhofer E**, **Verhey KJ.** Single molecule imaging reveals differences in microtubule track selection between Kinesin motors. *PLoS Biol* 7: e1000216, 2009. doi:10.1371/journal.pbio.1000216.
28. **Dompierre JP**, **Godin JD**, **Charrin BC**, **Cordelières FP**, **King SJ**, **Humbert S**, **Saudou F.** Histone deacetylase 6 inhibition compensates for the transport deficit in Huntington's disease by increasing tubulin acetylation. *J Neurosci* 27: 3571–3583, 2007. doi:10.1523/JNEUROSCI.0037-07.2007.
29. **Reed NA**, **Cai D**, **Blasius TL**, **Jih GT**, **Meyhofer E**, **Gaertig J**, **Verhey KJ.** Microtubule acetylation promotes kinesin-1 binding and transport. *Curr Biol* 16: 2166–2172, 2006. doi:10.1016/j.cub.2006.09.014.
30. **Eshun-Wilson L**, **Zhang R**, **Portran D**, **Nachury MV**, **Toso DB**, **Löhr T**, **Vendruscolo M**, **Bonomi M**, **Fraser JS**, **Nogales E.** Effects of α-tubulin acetylation on microtubule structure and stability. *Proc Natl Acad Sci USA* 116: 10366–10371, 2019. doi:10.1073/pnas.1900441116.
31. **Portran D**, **Schaedel L**, **Xu Z**, **Théry M**, **Nachury MV.** Tubulin acetylation protects long-lived microtubules against mechanical ageing. *Nat Cell Biol* 19: 391–398, 2017. doi:10.1038/ncb3481.
32. **Xu Z**, **Schaedel L**, **Portran D**, **Aguilar A**, **Gaillard J**, **Marinkovich MP**, **Théry M**, **Nachury MV.** Microtubules acquire resistance from mechanical breakage through intralumenal acetylation. *Science* 356: 328–332, 2017. doi:10.1126/science.aai8764.
33. **Olson AL**, **Trumbly AR**, **Gibson GV.** Insulin-mediated GLUT4 translocation is dependent on the microtubule network. *J Biol Chem* 276: 10706–10714, 2001. doi:10.1074/jbc.M007610200.
34. **Bertrand L**, **Ginion A**, **Beauloye C**, **Hebert AD**, **Guigas B**, **Hue L**, **Vanoverschelde J-L.** AMPK activation restores the stimulation of glucose uptake in an in vitro model of insulin-resistant cardiomyocytes via the activation of protein kinase B. *Am J Physiol Heart Circ Physiol* 291: H239–H250, 2006. doi:10.1152/ajpheart.01269.2005.
35. **Muretta JM**, **Romenskaia I**, **Cassiday PA**, **Mastick CC.** Expression of a synapsin IIb site 1 phosphorylation mutant in 3T3-L1 adipocytes inhibits basal intracellular retention of Glut4. *J Cell Sci* 120: 1168–1177, 2007. doi:10.1242/jcs.03413.
36. **Balteau M**, **Van Steenbergen A**, **Timmermans AD**, **Dessy C**, **Behets-Wydemans G**, **Tajeddine N**, **Castanares-Zapatero D**, **Gilon P**, **Vanoverschelde J-L**, **Horman S**, **Hue L**, **Bertrand L**, **Beauloye C.** AMPK activation by glucagon-like peptide-1 prevents NADPH oxidase activation induced by hyperglycemia in adult cardiomyocytes. *Am J Physiol Heart Circ Physiol* 307: H1120–H1133, 2014. doi:10.1152/ajpheart.00210.2014.
37. **Shaner NC**, **Campbell RE**, **Steinbach PA**, **Giepmans BNG**, **Palmer AE**, **Tsien RY.** Improved monomeric red, orange and yellow fluorescent proteins derived from Discosoma sp. red fluorescent protein. *Nat Biotechnol* 22: 1567–1572, 2004. doi:10.1038/nbt1037.
38. **Luo J**, **Deng Z-L**, **Luo X**, **Tang N**, **Song W-X**, **Chen J**, **Sharff KA**, **Luu HH**, **Haydon RC**, **Kinzler KW**, **Vogelstein B**, **He T-C.** A protocol for rapid generation of recombinant adenoviruses using the AdEasy system. *Nat Protoc* 2: 1236–1247, 2007. doi:10.1038/nprot.2007.135.
39. **Alrob OA**, **Sankaralingam S**, **Ma C**, **Wagg CS**, **Fillmore N**, **Jaswal JS**, **Sack MN**, **Lehner R**, **Gupta MP**, **Michelakis ED**, **Padwal RS**, **Johnstone DE**, **Sharma AM**, **Lopaschuk GD.** Obesity-induced lysine acetylation increases cardiac fatty acid oxidation and impairs insulin signalling. *Cardiovasc Res* 103: 485–497, 2014. doi:10.1093/cvr/cvu156.
40. **Haggarty SJ**, **Koeller KM**, **Wong JC**, **Grozinger CM**, **Schreiber SL.** Domain-selective small-molecule inhibitor of histone deacetylase 6 (HDAC6)-mediated tubulin deacetylation. *Proc Natl Acad Sci USA* 100: 4389–4394, 2003. doi:10.1073/pnas.0430973100.
41. **Geeraert C**, **Ratier A**, **Pfisterer SG**, **Perdiz D**, **Cantaloube I**, **Rouault A**, **Pattingre S**, **Proikas-Cezanne T**, **Codogno P**, **Poüs C.** Starvation-induced hyperacetylation of tubulin is required for the stimulation of autophagy by nutrient deprivation. *J Biol Chem* 285: 24184–24194, 2010. doi:10.1074/jbc.M109.091553.

42. **Renguet E**, **Bultot L**, **Beauloye C**, **Horman S**, **Bertrand L.** The regulation of insulin-stimulated cardiac glucose transport via protein acetylation. *Front Cardiovasc Med* 5: 70, 2018. [Erratum in *Front Cardiovasc Med* 5: 103, 2018].
43. **Yang J**, **Holman GD.** Insulin and contraction stimulate exocytosis, but increased AMP-activated protein kinase activity resulting from oxidative metabolism stress slows endocytosis of GLUT4 in cardiomyocytes. *J Biol Chem* 280: 4070–4078, 2005. doi:10.1074/jbc.M410213200.
44. **Rahmani S**, **Defferrari MS**, **Wakarchuk WW**, **Antonescu CN.** Energetic adaptations: metabolic control of endocytic membrane traffic. *Traffic* 20: 912–931, 2019. doi:10.1111/tra.12705.